

ICEMG 2023-XXXXX

BLDC motor behavior under PWM-MPC drive in unbalanced voltage conditions

Mohsen dashtbani¹, reza roshanfekr²

¹Hakim Sabzevari university, sabzevar; Mohsen.dashtbanie@gmail.com

¹Hakim Sabzevari university, sabzevar; r.roshanfekr@hsu.ac.ir

Introduction

Brushless direct current electric motors (BLDC) have high efficiency and accuracy, but the torque generated by these motors has a high ripple. One of the causes of torque ripple in these motors is stator current ripple, which improves by modifying the motor power supply. Major methods of improving the power effect of these motors require extensive and complex modifications to the drive structure of the motor and can be used in a certain range of speed and load torque [1].

Recently, a number of researchers have been able to improve the torque ripple caused by the power supply effect under different load torques and at different speeds by using a model called current predictive model. The design and implementation of this model is very simple and low cost and can be used in a wide range of motor speed and under different load torques [2].

Predictive control has long been used in fields other than power and drive electronics. The use of model predictive control (MPC) has been extended to applications related to power converters in the last 10 years due to its simple implementation and ability to handle multivariable [3]. The basis of this control is based on two key principles. One is the prediction of the state of the control system outputs through the prediction of system state changes (control variables) in the future, and the other is the process of optimizing the control system inputs to

achieve desired outputs. In simpler terms, this control method determines which option is the best option for the system to apply based on the user's command, so that in the future (one or more control intervals ahead), the error of the system outputs with the control will be less [4].

With the integration of MPC and PWM, a control system for BLDC motor has been designed, which can suppress the motor torque ripple caused by the ripple of the non-commutation phase current to a large extent at the moments of commutation. The working principles of this system are as follows: PWM pulses issue the motor drive switches whose reference signal is taken from a current PI controller that controls the error between the current of the next moment and the current of the power supply. At commutation moments, the PWM pulses issue the motor drive switches that its reference signal is issued from the MPC block, which creates this signal with the formulas mentioned in the MPC section. MPC, at the moments of commutation, by changing the duty cycle of the incoming and outgoing phase path switches, distortion occurs in Fig. It inhibits the torque ripple of the non-commutation phase current at commutation moment. The instantaneous current is generated through a speed PI controller that controls the error between the set point speed and the actual speed.

The use of PWM-MPC method in the drive of BLDC motors to control the ripple of the torque compared to similar methods has a much simpler structure and can be used at a lower cost. Also, this method has been able to achieve desired results in a wide range of motor speed and under different load torques [2].

One of the most important things in the design of motors and their drive is the proper behavior of the motor in the unbalanced conditions of the phase windings current. Studies show that the voltage imbalance in the motor can have many negative effects such as reducing the efficiency, increasing the temperature of the coil, reducing the life of the motor in its performance [5]. Therefore, it is very important to design the motor and its drive so that it can neutralize the negative effects of unbalanced motor windings current.

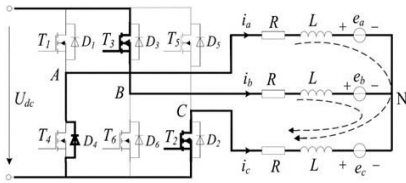
This paper explains the cause of torque ripple in the motor. The PWM-MPC method and how it works in controlling torque ripple is explained. The results of simulating the motor under drive with this method in terms of voltage balance and voltage imbalance are explained. The results show that using the predictive control system, the torque ripple is reduced to an acceptable level. It can be a good option for designing BLDC motor drives. The motor behaves well in unbalanced voltage conditions.

Commutation torque ripple

Ripple in the torque of brushless DC motors is mainly due to the following factors: cogging effect, Reluctance torque, power effect [6]. The cogging effect is caused by the interaction of the rotor magnetic flux and the stator reluctance changes [7]. Reluctance torque is caused by the interaction of stator electromagnetic forces with changes in the rotor's magnetic reluctance angles.

The effect of motor power is caused by the delay In reaching the maximum and minimum levels of stator currents due to inductance of stator windings. due to the difference in the slope rate of the currents involved in the commutation at the moment of commutation, distortion occurs in the form of the stator current. and due to the direct relationship between stator phase current and torque, this distortion directly leads to ripples in the electromagnetic torque of the motor[6].

for a deeper understanding of motor performance, commutation from the AC phase to the BC phase is considered as an example in this section. figure 1 shows the current path of the stator phase winding in this case. phase C acts as a non-involved phase in this commutation.the source current enters the motor phase A through D4 and after passing through the phase A windings, it enters phase C from the neutral point (the connection point of the three-winding star) and after passing through the phase C winding, it enters the source again through T2 and this shape closes the



circuit.

Figure 1. Current path from inverter switches to BLDC motor winding in commutation from AC phase to BC phase

Assuming that the back-EMF voltage is constant during commutation and equal to E, we will have a neutral point for the voltage.

$$u_N = \frac{U_{dc} - E}{3} \quad (1)$$

Assuming the stator phase winding is balanced, the inductance values and the resistance of the phases are assumed to be equal to each other.

$$i_a + i_b + i_c = 0 \quad (2)$$

Assuming that the three-phase windings of the motor are ideal (value R = 0) and enter the algebraic sum equation of the three-phase currents (Eq. 2) and the neutral point voltage (Eq. 1) in the equations of the motor circuit model, the equation of the slope rate of the three-phase currents is as follows:

$$\begin{cases} \frac{di_a}{dt} = \frac{-U_{dc} - 2E}{3L} \\ \frac{di_b}{dt} = \frac{2U_{dc} - 2E}{3L} \\ \frac{di_c}{dt} = \frac{-U_{dc} + 4E}{3L} \end{cases} \quad (3)$$

According to the slope rate of three-phase currents during commutation from phase A to phase B, three general conditions can occur:

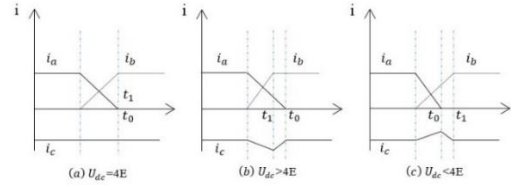


Figure 2. Current path from inverter switches to BLDC motor winding in commutation from AC phase to BC phase

t0 = time when the output phase current reaches zero

t1 = time when the input phase current reaches the maximum value

According to the assumptions made for the electromagnetic torque of the motor, Equation 4 is established.

$$T_e = \frac{1}{\omega_r} (e_a \cdot i_a + e_b \cdot i_b + e_c \cdot i_c) \quad (4)$$

Where T_e is Electromagnetic torque of the motor and ω_r is mechanical speed of the rotor.

At the time of commutation, all three phases windings may be current carriers. However, due to the symmetry equation of the currents, the amount of single-phase current can be obtained from the other two phases.

$$T_e = \frac{e_a i_a + e_b i_b}{\omega_m} = (2 * E i_c) / \omega_m \quad (5)$$

Equation 5 also shows the mechanical equation of the BLDC motor

$$T_e - T_L = J \frac{d\omega_r}{dt} + B \omega_r \quad (6)$$

Where T_L is load torque and J is inertia and B is friction coefficient.

Equation 5 shows the dependence of the motor electromagnetic torque on the stator single-phase current. With this description, any oscillation in the stator phase current waveform will directly lead to oscillation in the electromagnetic torque waveform.

Table 1. motor torque ripple in three commutation modes

state	ia-ib fall/raise rate	t0-t1 relationship	BackEMF-Udc relationship	Current-torque ripple
1	$\frac{di_a}{dt} = \frac{di_b}{dt}$	t0=t1	Udc=4E	Not ripple
2	$\frac{di_a}{dt} < \frac{di_b}{dt}$	t0>t1	Udc>4E	Convex ripple
3	$\frac{di_a}{dt} > \frac{di_b}{dt}$	t0<t1	Udc<4E	Concave ripple

By using the methods of reducing the ripple due to feeding, by converting the states b and c to a, the electromagnetic torque ripple of the motor can be traditional Methods for reducing the torque ripple due to the effect of power supply require fundamental changes in the power supply circuits and the structure of the inverter and complex and cumbersome calculations, and are mainly useful in low or high speed range and do not include a wide speed range. Implementing these methods is very time consuming and costly due to the fundamental modifications in the design of the controller. Therefore, it is important to find a way to change the overall structure of the motor controller and simply integrate a controller that can inhibit torque ripple in moments of commutation.

PWM-MPC

The proposed method in this project to reduce current ripple is to integrate bandwidth modulation and predictive control system (PWM-MPC). In this method, by changing the duty cycle of the switches in the flow path of the incoming and outgoing phases during commutation based on the predictive control system, the current ripple involved in commutation can be reduced at commutation moments. The results show that the phase ripple of the phase not involved in commutation and the torque ripple at the commutation moments are significantly reduced using this method [4].

In the commutation process from AC phase to BC phase, we have the following equations with the definition of DB as a phase B power switch of phase B [1].

$$\begin{cases} u_A = R i_a + L \frac{d i_a}{d t} + e_a + u_N = 0 \\ u_B = R i_b + L \frac{d i_b}{d t} + e_b + u_N = D_B \times U_{dc} \\ u_c = R i_c + L \frac{d i_c}{d t} + e_c + u_N = 0 \end{cases} \quad (7)$$

Udc>4E

Assuming the back EMF (120 ° trapezoid) waveform is ideal:

$$E_a = E_b = E, \quad E_c = -E \quad (8)$$

And according to Eq. (2) and Eq. (7) mentioned can be harvested:

$$u_{BC} = -3L \frac{d i_c}{d t} - 3R i_c + 4E = D_B \times U_{dc} \quad (9)$$

By defining d0 as the diode cycle switch, input phase current (B) and using the Euler forward method.

$$d_0 = \frac{3L}{T_s} \{ [i(k+1) - i(k) + 3Ri(k) + 4E(k)] / U_{dc} \} \quad (10)$$

Where Ts is equal to the sample period. I (k) is the non-commutation current at the moment k and i (k+1) is the non-commutation current at the next moment.

Assuming that the non-commutation current is constant and matches the predicted current with the given current, which is equal to the output current in the closed-loop system, the velocity at the moment k:

$$i(k+1) = i^*(K) \quad (11)$$

Udc<4E

In the commutation process from AC phase to BC phase, we have the following relations with the definition of DA

as the power cycle switch of phase A[8]:

$$\begin{cases} u_A = R i_a + L \frac{d i_a}{d t} + e_a + u_N = D_A \times U_{dc} \\ u_B = R i_b + L \frac{d i_b}{d t} + e_b + u_N = 0 \\ u_c = R i_c + L \frac{d i_c}{d t} + e_c + u_N = 0 \end{cases} \quad (12)$$

And according to Eq. (2) and Eq. (12) mentioned can be harvested:

$$u_{AC} = -3L \frac{d i_c}{d t} - 3R i_c + 4E = D_A \times U_{dc} \quad (13)$$

By defining d1 as the diode cycle switch, output phase current in the commutation using the Euler forward method.

$$d_1 = \frac{3L}{T_s} \{ [i(k+1) - i(k) + 3Ri(k) + 4E(k) - U_{dc}] / U_{dc} \} \quad (14)$$

Where Ts is equal to the sample period, i(k) is the non-commutation current at the moment k and i(k+ 1) is the non-commutation current at the next moment.

As a result, the PWM-MPC method can effectively limit the current ripple and consequently the torque ripple by changing the diode cycle of the input and output current path switches.

Simulation of case study

Figure 3 shows the general simulation of the project. This method uses three sensors. The first sensor is the Hall effect sensors, which report rotor status and motor speed, the second sensor is the DC source current sensor, which reports the source current, and the third sensor is the three-phase current sensor, which reports the stator phase current.

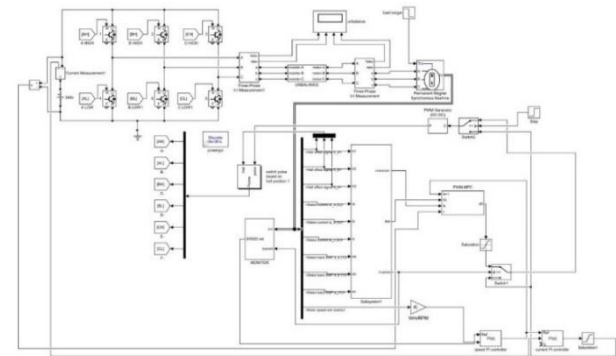


Figure 3. Simulation of PWM-MPC model in Simulink environment

In this control system, the block detection of commutation moments, by receiving the values of Hall effect sensors and three-phase current, detects the commutation moments and the phase current not involved in the commutation. Speed Detection Block detects the motor speed according to the output of the Hall effect sensors and issues the amount of anti-drive force at any moment with a constant gain of the anti-drive force. The proportional integral motor speed regulator receives the set speed applied by the user and compares its instantaneous value with the actual value of the reference current speed, and the proportional

integral flow regulator compares the reference current with the actual current, the reference signal. Creates a PWM block. This block issues the commands of the switches according to the commutation table according to the status of the Hall effect sensor signals and the reference signal received from the current controller. The PWM-MPC block, according to the values of the anti-excitation force and the current of the phase not involved in the commutation at any moment, the values of the duty cycle switch output the path of the phases involved in the commutation. A switch is located in the output path of the current controller, which in times of commutation takes the values of the cycle from the PWM-MPC block and in other moments uses the output of the current controller. The output duty cycle values are passed to the PWM-generator block and pulses are generated. These pulses go to the vector selection table block, and this block emits the appropriate signal to the inverter power switches according to the values of the Hall effect sensors and the input pulse values.

The simulation of this model has been done in Simulink environment of MATLAB 2017 software. The parameters included in the design are as shown in Table 2.

Table 2. BLDC simulation parameters

parameter	value
Rated voltage(V)	240
Phase resistance(Ω)	0.75
Phase inductance(mH)	1.048
Pole-pair	2
Load torque(N.m)	1-2-5
Intertia	0.06
Viscous damping	5e-6

Balance voltage

Figure 4 shows the performance of the motor at 500 rpm and under a load torque of 1 Nm as an example. The upper side of the image shows the moments of commutation. The second part shows the single-phase current waveform of the stator and the lower part shows the electromagnetic torque of the motor.

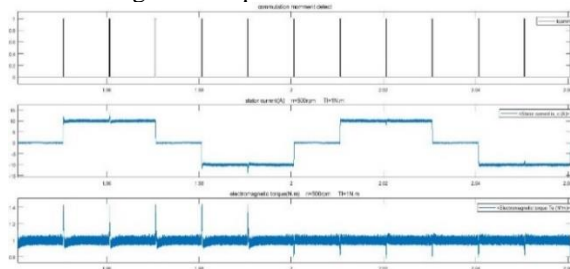


Figure 4- Commutation moment diagram, stator single-phase current waveform, motor torque at 500 rpm and under load torque 1 N.M. PWM-MPC applied from second 2

As can be seen in Figure 4, the protrusion in the stator phase current waveform occurred exactly at the moment of commutation and at exactly the same moment it led to the protrusion in the waveform of the motor electromagnetic torque. After the second, with the introduction of the current forecasting control system, the protrusion of the current waveform is drastically

reduced, and this has led to a reduction of the protrusion in the electromagnetic torque waveform of the motor

Comparison of simulation results with practical experiment of reference paper in balance voltage state

In this section, in order to validate the simulation results, the waveforms obtained in Section 4.1 under the same conditions are compared with the results obtained from the practical test in the reference paper. Author of the reference paper measured stator phase current and electromagnetic torque of the motor at two speeds of 500 and 1500 rpm and under load torque of 0.1 Nm. Figures 5 (a, b, c and d) and Fig. 6 (a, b, c and d) show a comparison of these two waveforms with the simulation results.

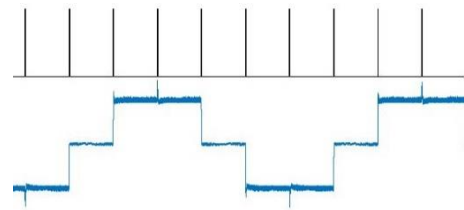


Fig. 5 (a) stator current wave form in simulation at 500RPM 0.1N.M using traditional method

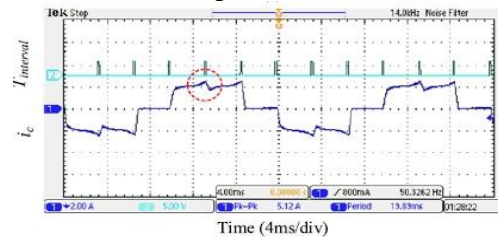


Fig. 5 (b) stator current wave form in real experience at 500RPM 0.1 N.M using traditional method

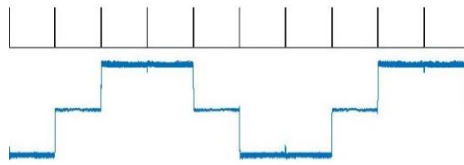


Fig. 5 (c) stator current wave form in simulation at 500 RPM 0.1N.M. using PWM-MPC method

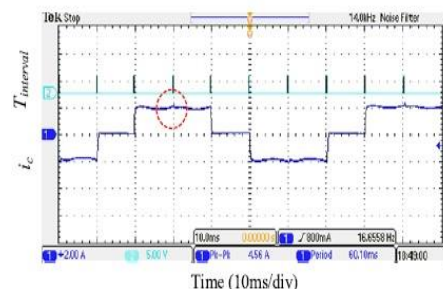


Fig. 5 (d) stator current wave form in real experience at 500RPM 0.1 N.M using PWM-MPC method

Figure 5- comparison current wave form between simulation and real experience results at 500 RPM, 0.1 N.M.

As shown in Fig. 5 (a, b, c and d), PWM-MPC method has been able to significantly reduce the amount of torque ripple caused by stator current ripple at commutation moments at 500RPM speed and under 0.1

N.M. torque load, both in simulation and practical experiments.

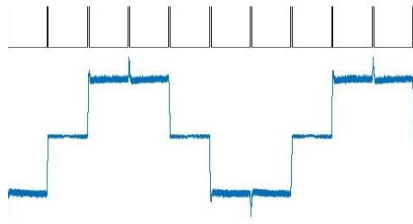


Fig. 6 (a) stator current wave form in simulation at 1500RPM 0.1N.M. traditional method using traditional method

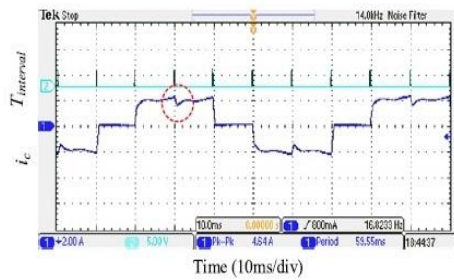


Fig. 6 (b) stator current wave form in real experience at 1500RPM 0.1 N.M using traditional method

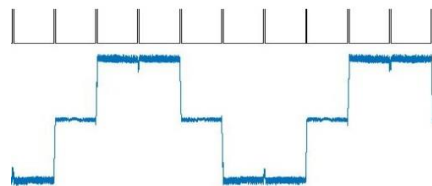


Fig. 6 (c) stator current wave form in simulation at 1500 RPM 0.1 N.M. using PWM-MPC method

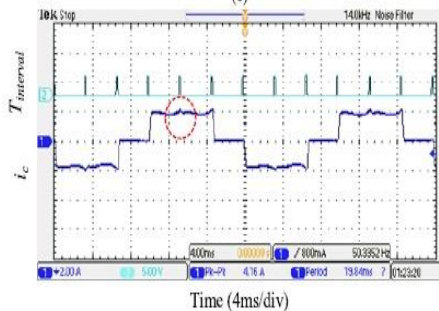


Fig. 6 (d) stator current wave form in real experience at 1500RPM 0.1 N.M using PWM-MPC method

Similar to Fig. 5, PWM-MPC method has been able to significantly reduce the amount of torque ripple caused by stator current ripple at commutation moments at 1500 RPM speed and under 0.1 N.M. torque load, both in simulation and practical experiments.

Therefore, it can be concluded that this technique is able to reduce the torque ripple caused by the stator current ripple at commutation moments at high and low speeds.

Imbalance voltage

In this section, motor performance under three-phase voltage and current unbalanced conditions is simulated in MATLAB Simulink environment and the results of

this simulation are compared with motor simulation results under three-phase voltage and current balance conditions. Results for 1500 rpm and 2 N.M. load torque.

In order to create an imbalance, resistance is used in series with the output of the three-phase inverter and the three-phase winding of the motor. The experiment is repeated in two cases of unbalance of one-phase voltage compared to the other two phases (Two of the three phases are balanced) and voltage imbalance of all three phases and the results are reported.

To investigate the one-phase unbalance of three phases, we set the resistance value of phase A to three times the internal resistance of the winding of phase A to 2.25 ohms and the resistance of phase C to zero.

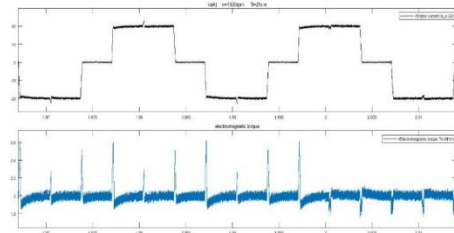


Figure 7- One-phase stator current waveform and motor electromagnetic torque under unbalanced phase A current condition. PWM-MPC employed from second 2

Figure 7 shows the one-phase current of the motor stator and the electromagnetic torque of the motor under unbalanced conditions of the single-phase current of the three-phase motor. Torque ripple values in unipolar conditions of single-phase three-phase current are 9.6951% for PI-PWM system and 7.2573% for PWM-MPC system.

Comparison of torque ripple percentages in unbalanced state and study of waveforms in these two states shows that the use of predictive system has been able to correct the torque ripple caused by stator phase current ripple in unbalanced single-phase current of three phases.

Voltage imbalance of three phases

To investigate the current imbalance of all three phases, we set the value of phase A resistance to twice the internal resistance of phase A winding equal to 1.5 ohms and the resistance of phase C to the internal resistance of phase C winding equal to 0.75 ohms.

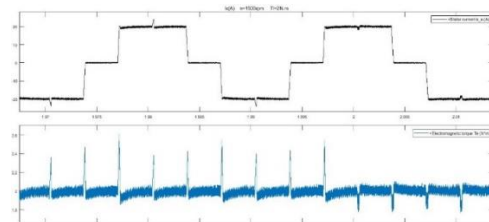


Figure 8- one-phase stator current waveform and electromagnetic torque of motor under unbalanced three-phase current conditions. PWM-MPC applied from second 2

second 2

Figure 8 shows the one-phase current of the motor stator and the electromagnetic torque of the motor under the unbalanced conditions of the three-phase motor current. Torque ripple values in three-phase unbalanced current conditions are 9.5% for the PI-PWM system and 7.2375% for the PWM-MPC system.

Comparison of the percentage of torque ripple in the unbalanced state and the study of waveforms in these two states show that the use of the prediction system has been able to correct the torque ripple caused by the stator phase current ripple in the three-phase unbalanced state.

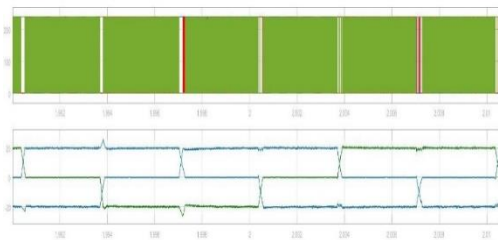


Fig. 9 (a)- Three-phase voltage and current waveform before and after unbalanced application of single-phase three-phase current PWM-MPC applied from second 2

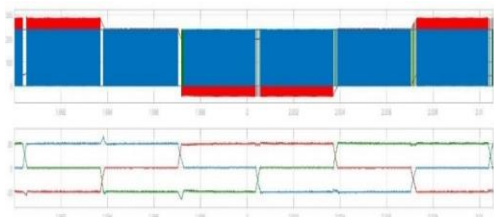


Figure 9- (b) Three-phase voltage and current waveform before and after unbalanced application of three-phase current PWM-MPC applied from second 2

Figure 9 shows the three-phase motor voltage and current waveform in balanced condition and in unbalanced single-phase and three-phase currents. From 2 seconds the forecasting system enters the circuit. Examining the shapes, we see that the current waveforms before and after the unbalanced application are not different, but in the case of voltages, the voltage amplitude of all three phases is equal in balanced condition, and then in the unbalanced state of the single-phase current, the single-phase voltage range with the other two phases. It is different and in the unbalanced state of three-phase current, the voltage range of all three phases is different from each other. Applying the predictive control system after 2 sec. had no effect on the unbalanced phase voltage range, but improved the current at ripple commutation moments in the current waveform.

Conclusions

Various methods have been designed, tested, and operated to overcome the high torque ripple in BLDC motors, which generally require extensive modifications to the motor drive structure and can be operated at a certain range of speed and under specific load torque.

The simulation results show that using PWM-MPC method has been able to significantly reduce the stator phase current ripple and consequently the electromagnetic torque ripple of the motor at commutation moments, leading to increased motor efficiency and life and reduced unwanted vibrations and noise.

Predictive control system can also play an effective role in reducing motor torque ripple at commutation moments in unbalanced single-phase or multi-phase current conditions of BLDC motor.

References

- [1] K. Xia, Y. Ye, J. Ni, Y. Wang, P. Xu, "Model predictive control method of torque ripple reduction for BLDC Motor," *IEEE Trans. Magn.*, Vol. 56, No. 1, pp. 1-6, 2020.
- [2] K. Xia, Y. Ye, Y. Tian, M. Xu, Y. Tang, "The model predictive control method of torque ripple reduction for BLDC motor," in *2018 Asia-Pacific Magnetic Recording Conference, APMRC 2018*. Shanghai, China, 2018.
- [3] R. Ramírez C. R. Baier, J. Espinoza, F. Villarroel, "Finite control set MPC with fixed switching frequency applied to a grid connected single-phase cascade h-bridge inverter," *Energies*, Vol. 13, No. 20, pp. 1-18, 2020.
- [4] M. Lei, Y. Zhang, L. Meng, Y. Wang, Z. Yang, "A Novel Adaptive Model Predictive Control Based Three-Phase Inverter Current Control Method," *Applied Sciences*, Vol. 9, pp. 1-18, 2019.
- [5] C. Y. Lee, W. J. Lee, "Effects of nonsinusoidal voltage on the operation performance of a three-phase induction motor," *IEEE Trans. Energy Convers.* Vol. 14, No. 2, pp. 193-200, 1999.
- [6] M. Sumega, S. Zoššák, P. Varecha, P. Rafajdus, "Sources of torque ripple and their influence in BLDC motor drives," *Transportation Research Procedia*. Vol. 40 pp. 519-526., 2019.
- [7] Y. Ozoglu, "New stator tooth for reducing torque ripple in outer rotor permanent magnet machine," *Advanced Electr. Comput. Eng.*, Vol. 16, No. 3, pp. 49-56, 2016.
- [8] Y. Mandel, G., "Weiss Reduction of torque ripple in brushless DC motor drives," *IFAC Proceedings Volumes*. Vol. 42, pp. 84-89, 2009.